Biochimica et Biophysica Acta 861 (1986) 44–52
Elsevier

BBA 73156

Methyl group substitution at C(1), C(2) or C(3) of the glycerol backbone of a diether phosphocholine: a comparative study of bilayer chain disorder in the gel and liquid-crystalline phases

E. Neil Lewis [a], Robert Bittman [b] and Ira W. Levin [a]

[a] *Laboratory of Chemical Physics National Institute of Arthritis, Diabetes and Digestive and Kidney Diseases, National Institutes of Health, Bethesda, MD 20892 and*
[b] *Department of Chemistry, Queens College of the City University of New York, Flushing, NY 11367 (U.S.A.)*

(Received 22 April 1986)

Key words: Ether-linked phospholipid; Raman spectroscopy; Intermolecular disordering; *trans / gauche* Isomerization; Bilayer structure; Phase transition

Alterations in the inter- and intramolecular packing characteristics of aqueous dispersions of methyl derivatives of di-*O*-hexadecylglycerophosphocholine (DHPC), an ether lipid in which the methyl group is substituted at the 1, 2 or 3 position of the glycerol backbone, were monitored by changes in the vibratioal frequencies and intensities of selected spectral features by Raman spectroscopy. Temperature profiles constructed from spectra reflecting intermolecular order / disorder rearrangements (C–H stretching mode region) and intramolecular order / disorder processes (C–C stretching mode region) provide insight into several important structural properties of diether lipid bilayers. The introduction of a methyl group into any position of the glycerol backbone alters both the characteristics of the DHPC pretransition and the temperature of the gel to liquid-crystalline phase transition. The main gel to liquid-crystalline phase transitions are 42.8°C in the pure diether lipid, 41.6°C for 3-Me-DHPC, 40.5°C for 2-Me-DHPC and 38.1°C for 1-Me-DHPC. Temperature profiles indicate that the degree of disordering for both the gel and liquid-crystalline states follows the sequence 2-Me-DHPC < 3-Me-DHPC < DHPC < 1-Me-DHPC. Phase transition widths, ΔT, determined from the spectroscopic temperature profiles, are discussed in terms of van't Hoff enthalpy functions involving both interchain and *trans / gauche* effects.

Introduction

Although ether phospholipids are widely distributed in a variety of biological membranes [1], a detailed knowledge of the effects of the linkage on the structural and dynamical behavior of bilayer assemblies is limited. This is in sharp contrast to our understanding of the membrane properties of the more ubiquitous acyl phospholipids. Recent physical studies on model and reconstituted ether- and ester-derived phospholipid bilayers have shown the differences in, for example, their thermal behavior, diffusion characteristics and intermolecular interactions with other membrane constituents [2–7]. Of particular structural relevance regarding either-linked phospholipids is the inference from recent X-ray diffraction data [8] that hydrated bilayers of 1,2-di-*O*-hexadecyl-*sn*-glycerol-3-phosphocholine (DHPC) exhibit a novel, interdigitated hydrocarbon chain arrange-

Abbreviation: DHPC, dihexadecylglycerophosphocholine.

Correspondence address: Laboratory of Chemical Physics National Institute of Arthritis, Diabetes and Digestive and Kidney Diseases, National Institutes of Health, Bethesda, MD 20892, U.S.A.

ment for gel-phase temperatures below the 35°C pretransition. In addition, ^{31}P nuclear magnetic resonance studies [8] suggest that long axis diffusion persists to lower temperature in DHPC dispersions in comparison to its acyl lipid counterpart, 1,2-dipalmitoylphosphatidylcholine (DPPC). Since substitution of ether linkages for the acyl moieties within the interface region of the phospholipid molecule significantly alters fundamental bilayer properties, it is pertinent to examine bilayer behavior as a consequence of introducing other structural modifications to the ether lipid at its headgroup/hydrocarbon chain boundary. There is a particular interest in describing the resulting conformational changes and chain-disordering effects propagated to the hydrophobic region of the lipid bilayer.

The present study examines by Raman spectroscopy the thermal behavior or aqueous multilamellar dispersions of DHPC in which a methyl group has been substituted at either the C(1), C(2) or C(3) position of the interfacial glycerol group. Alterations in the bilayer packing characteristics resulting from either intrinsic or extrinsic disruptive influences are sensitively monitored by changes in the vibrational Raman frequencies, intensities and bandwidths of selected spectral features [9,10]; in particular, specific spectral intervals reflect structurally distinct regions of the phospholipid molecule. Although the vibrational technique offers information on the origin of a variety of structural reorganizations within the lipid bilayer, we focus in this investigation on spectral intervals and features primarily reflecting changes in alkyl chain packing characteristics (2800–3100 cm^{-1} region) and *trans/gauche* conformational changes (1000–1200 cm^{-1} region). The peak-height intensity ratios I_{2935}/I_{2882} and I_{2847}/I_{2882} generally reflect the interchain order/disorder process, while changes in the I_{1086}/I_{1131} peak height ratios are related more directly to intrachain conformational changes [3,9].

Experimental procedures

DHPC was purchased from Calbiochem-Behring and used without further purification after the purity of the polycrystalline material had been checked spectroscopically. The 1- and 3-methyl-substituted derivatives of DHPC were synthesized as described previously [11]. The method for preparing the 2-methyl derivative will be described elsewhere (unpublished data). The criteria for ascertaining purity involved principally elemental analyses and proton NMR procedures. All three lipid systems were prepared as multilamellar assemblies. Aqueous dispersions were prepared by suspending DHPC (30 wt%) in distilled water in Kimex glass capillary tubes followed by mechanical agitation at 50°C for several minutes. The capillary tube were then sealed, packed in a bench-top clinical centrifuge and incubated at −14°C for several days.

Raman scattered radiation was collected from the incident 514.5 nm exciting line of a Coherent Radiation CR-3 laser delivering 200 mW of power at the sample. Spectra were acquired by a Spex Ramalog 6 spectrometer described previously [12]. Between eight and thirty signal-averaged scans were acquired for each spectrum at a scan rate of 1 $cm^{-1} \cdot s^{-1}$ in the 2800–3100 cm^{-1} and 1000–1200 cm^{-1} spectral intervals using a Nicolet NIC-1180 data system. Spectral frequencies, calibrated with atomic argon lines, are reported to ± 2 cm^{-1}. Temperature profiles were obtained in an ascending mode at 1.5–2 Cdeg intervals, allowing 15-min equilibration times between consecutive points. Uncertainties in the gel to liquid-crystalline phase-transition tempeatures derived from the various temperature-dependent intensity ratios range statistically from (± 0.1 to ± 1.0 Cdeg (see Table I).

Results

Representative spectra for 1-Me-DHPC, 2-Me-DHPC, 3-Me-DHPC and DHPC, recorded in the C-H stretching mode region (2800–3100 cm^{-1}) at comparable temperatures above and below their respective main phase transition, are shown in Fig. 1. Temperature profiles, constructed for the 1-, 2- and 3-Me-DHPC derivatives and for pure DHPC using the three spectral peak-height intensity ratios I_{2935}/I_{2882}, I_{2847}/I_{2882} and I_{1086}/I_{1131}, are presented in Figs. 2–4. Although the peak-height frequencies change with temperature, the low-temperature gel-phase values are used when reference is made to a specific ratio in either the figure

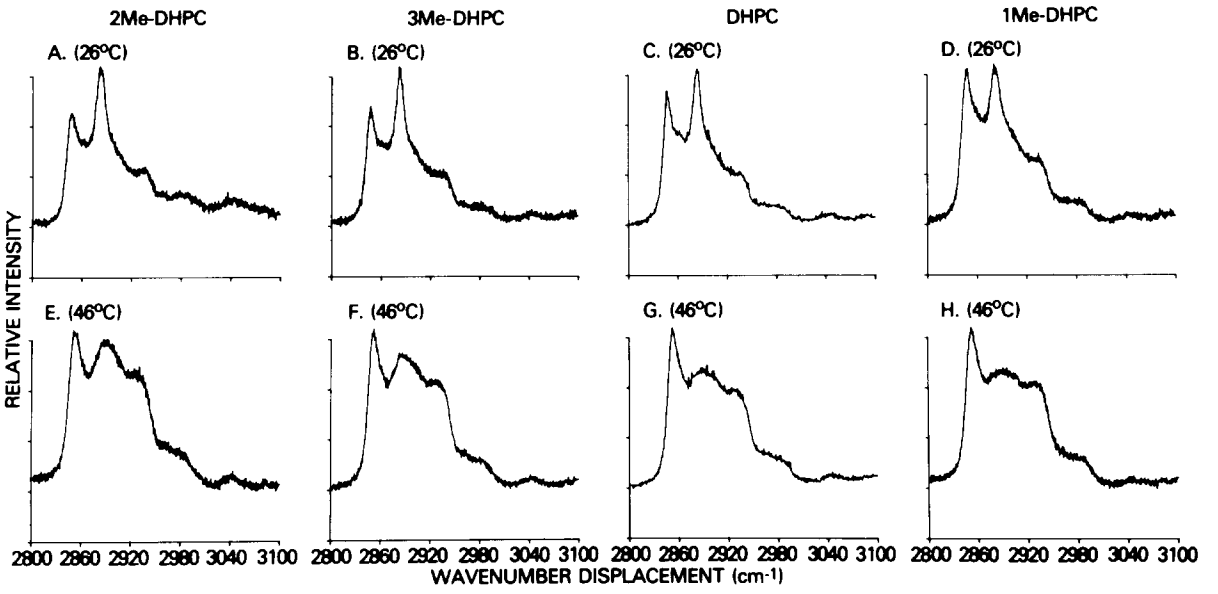

Fig. 1. Comparisons between the relative gel-phase order (A–D) and liquid-crystalline phase disorder (E–H) for aqueous dispersions of 2-Me-DHPC, 3-Me-DHPC, DHPC and 1-Me-DHPC. (Unsubstituted DHPC manifests a significant gel and liquid-crystalline phase polymorphism.)

legends or in the text. The basis for the vibrational assignments of these various modes has been previously discussed in detail (Ref. 9 and references contained therein). Briefly, the 2847, 2882 and 2935 cm^{-1} bands are assigned, respectively, to the hydrocarbon chain methylene C–H symmetric stretching modes, the methylene C–H asymmetric stretching modes and a Fermi resonance component of the chain terminal methyl C–H symmetric stretching mode superimposed upon additional methylene Fermi resonance components. The latter transitions involve Fermi resonance interactions between the manifold of overtones of the methylene deformation modes, defined by an appropriate vibrational phase angle, and the fundamental methylene symmetric stretching vibrations. The 1131 cm^{-1} feature represents the hydrocarbon chain all-*trans* C-C stretching mode, while the band at approx. 1086 cm^{-1} arises from the introduction of *gauche* conformers within the *trans* chain segments.

The three separate intensity ratios applied to the four samples in the 23–50°C temperature range display the characteristic profiles associated with phospholipids as they undergo the main gel to liquid-crystalline phase transition. For the I_{2935}/I_{2882} intensity ratio, the intensity parameter shown in Fig. 2 which reflects primarily interchain order/disorder processes with some superposition of intrachain disorder [12], the 2-Me-DHPC dispersion assumes the most highly ordered bilayer arrangement; the 1-Me-DHPC dispersion represents the most disordered bilayer in both the gel and liquid-crystalline phases. The 3-Me-DHPC and pure DHPC bilayers have similar profiles lying between these two limiting curves. Inspection of the temperature profiles derived from the I_{2847}/I_{2882} intensity ratios displayed in Fig. 3 indicates a somewhat different sequence. That is, although the pattern for the gel state for the methyl-substituted samples is the same as that measured by the I_{2935}/I_{2882} ratio, the liquid-crystalline phases of both pure DHPC and 1-Me-DHPC appear to be the most disordered in the series. We note that in some circumstances the I_{2847}/I_{2882} intensity ratio reflects more directly the lateral chain-chain interactions.

Fig. 4 displays the four temperature profiles constructed from the I_{1086}/I_{1131} spectral peak-height intensity ratios. This intensity ratio provides a direct measure of the degree of *trans/gauche* isomerization induced along the alkyl chain

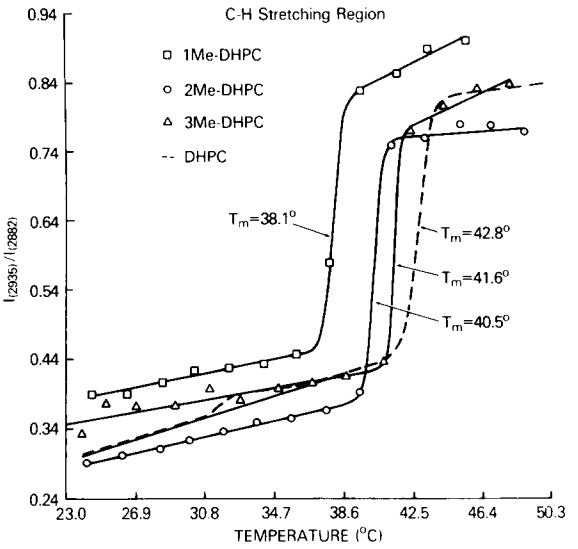

Fig. 2. Temperature profiles, derived from C–H stretching mode parameters, for methyl-substituted DHPC dispersions in excess water. Raman spectral peak height intensity ratios I_{2935}/I_{2882} were used as indices to characterize the thermal behavior of the hydrocarbon region of the liposomes. The dotted line reflects one of the possible polymorphic forms of DHPC bilayers.

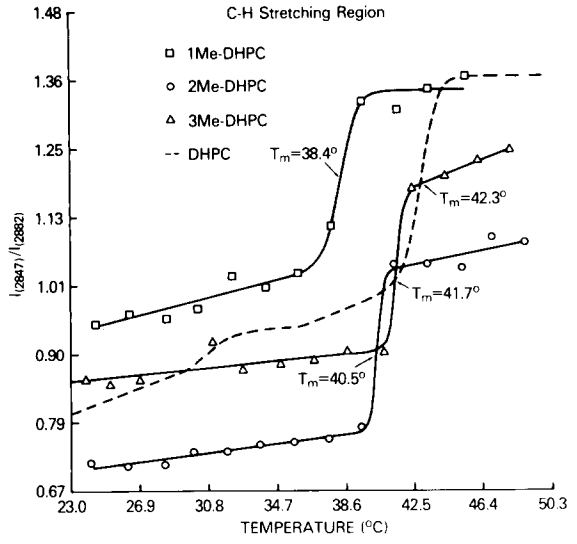

Fig. 3. Temperature profiles, derived from C–H stretching mode region parameters, for methyl-substituted DHPC dispersions in excess water. Raman spectral peak height intensity ratios I_{2847}/I_{2882} were used to characterize the thermal behavior of the hydrocarbon region of the liposomes. The dotted line reflects the same polymorphic form of DHPC delineated in Figs. 2 and 4.

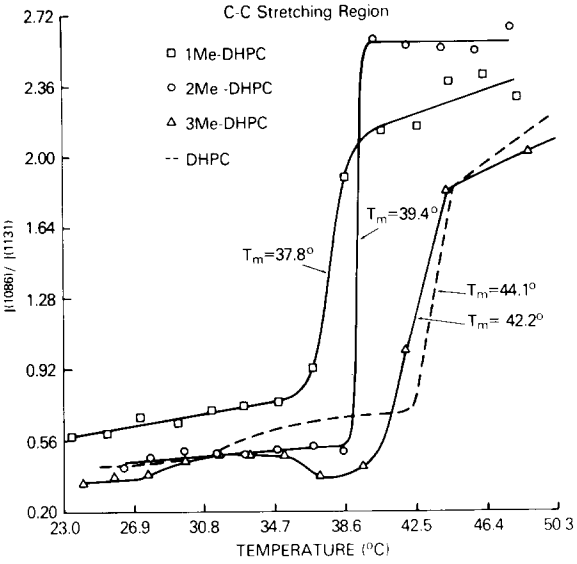

Fig. 4. Temperature profiles for methyl-substituted DHPC dispersions using the I_{1086}/I_{1131} (I_{gauche}/I_{trans}) intensity ratios as indices. The dotted line reflects the same polymorphic form of DHPC delineated in Figs. 2 and 3.

both above and below the main phase transition, T_m. This profile set indicates that, as before, the 1-Me-DHPC derivative is the most disordered in the gel state. Although the 2- and 3-Me-DHPC dispersions are approximately of equal order in the gel phase, 2-Me-DHPC exhibits the most intrachain disorder in the liquid-crystalline form, even more so than 1-Me-DHPC, which possesses the greatest interchain disorder (Fig. 3). This polymorphic form of unsubstituted DHPC is more intramolecularly disordered in the gel state at temperatures about 10 Cdeg below T_m than either 2- or 3-Me-DHPC (Fig. 4), but only exhibits as much intrachain disorder as 3-Me-DHPC in the liquid-crystalline phase.

Values for the widths of the transition intervals, ΔT, which give an indication of the cooperativity of the chain melting during the phase transition, correlate well with the degree of interchain ordering observed for the bilayers using the I_{2847}/I_{2882} ratios. These data are summarized in Table I with the observed values for T_m. The T_m and ΔT values are determined systematically by a least-squares fitting of the intensity ratios to an analytical expression reflecting a two-state model for the gel to

liquid-crystalline phase transition [13]. The uncertainties tabulated for T_m in Table I reflect the least-squares estimates. Values for ΔT increase from approx. 1.5 to 4.1 Cdeg, in accord with the degree of disordering observed for the gel phase, particularly, and the liquid-crystalline states, generally, in the sequence:

2-Me-DHPC < 3-Me-DHPC < DHPC < 1-Me-DHPC

The correlation between values of ΔT and the other two intensity order/disorder parameters (I_{2935}/I_{2882} and I_{1086}/I_{1131}), however, is not so clearly defined. For all the intensity ratios examined, the smallest values of ΔT, reflecting the most cooperative phase transition, was observed for 2-Me-DHPC.

Vibrational frequencies measured for these bilayer systems in both the gel and liquid-crystalline states in all cases indicate an increase in frequency of approx. 5 and 7 cm^{-1}, respectively, for the bands at 2847 and 2882.5 cm^{-1} (Fig. 1) as the smples pass through the phase transition. These bands, as noted above, are assigned to alkyl chain methylene symmetric and asymmetric stretching modes, respectively. The frequency measured for the band centered at approx. 2935 cm^{-1}, which is attributed, in part, to the chain terminal methyl stretching mode, increases by about 2 cm^{-1} for 2-Me-DHPC and 3-Me-DHPC as these dispersions pass through the phase transition, but decreases approx. 2 cm^{-1} for 1-Me-DHPC. Comparisons of the carbon-carbon (C–C) stretching mode frequencies for the gel and liquid-crystalline phases for the three methyl-substituted samples reveal the following pattern. The strong band centered at approx. 1063.5 cm^{-1}, associated with the all-*trans* out-of-phase skeletal chain motion, increses in frequency by about 2 cm^{-1} as the samples pass through the main phase transition. The band centered at approx. 1131 cm^{-1}, attributed to the in-phase C–C motion for the all-*trans* chain segments, however, decreases in frequency by about 1 cm^{-1} above T_m in all cases. The frequency of the band assigned to the presence of *gauche* conformers at about 1087 cm^{-1} in the gel phase for both 2- and 3-Me-DHPC, decreases by about 5 cm^{-1} to 1082 cm^{-1} for 3-Me-DHPC in the liquid-crystalline form, but remains practically unaltered for 2-Me-DHPC above T_m. For 1-Me-DHPC, however, the band associated with *gauche* conformers at 1083.5 cm^{-1} in the gel phase increases in frequency by approx. 2 cm^{-1} above T_m. The differences in the *gauche* frequency marker in the lipid series may reflect varying distributions of *gauche* conformers within the chain regions both distal and proximal to the glycerol backbone.

A further modification of the melting behavior of these diether lipids by the introduction of methyl groups is the effects of substitution on the pretransition. Pure DHPC has a clearly defined pretransition as measured by all three temperature profiles (Figs. 2–4) at 31°C, whereas a suggestion of the pretransition is perhaps discernible only for the 1- and 3-Me-DHPC dispersions using the I_{2847}/I_{2882} intensity ratios, the spectral parameters most sensitive to this lattice reorganization. A broad pretransition is observed, however, for 3-Me-DHPC using the intensity ratio derived from the C–C stretching mode region. All three intensity parameters suggest elimination of the pretransition for 2-Me-DHPC.

TABLE I

SUMMARY OF THE THERMAL DATA FOR THE VARIOUS BILAYER SYSTEMS OF DHPC AND ITS METHYL DERIVATIVES DERIVED FROM RAMAN SPECTRAL PARAMETERS

Thermal data (T_m and ΔT) were determined from a least-squares fit to a two-state model for the gel and liquid-crystalline phase transition [14]. T_m represents the main phase transition, while ΔT represents the phase-transition breadth.

	Raman intensity index	T_m (°C)	ΔT (Cdeg)
1-Me-DHPC	I_{2935}/I_{2882}	38.1 ± 0.1	< 2.2
	I_{2847}/I_{2882}	38.4 ± 0.2	< 4.1
	I_{1086}/I_{1131}	37.8 ± 0.1	2.1 ± 0.4
2-Me-DHPC	I_{2935}/I_{2882}	40.5 ± 0.1	1.2 ± 0.1
	I_{2847}/I_{2882}	40.5 ± 1.0	< 1.5
	I_{1086}/I_{1131}	39.4 ± 1.0	< 1.1
3-Me-DHPC	I_{2935}/I_{2882}	41.6 ± 0.9	< 1.4
	I_{2847}/I_{2882}	41.7 ± 0.9	< 1.9
	I_{1086}/I_{1131}	42.2 ± 0.2	< 5.3
DHPC	I_{2935}/I_{2882}	42.8 ± 0.2	< 3.4
	I_{2847}/I_{2882}	42.3 ± 1.0	< 4.0
	I_{1086}/I_{1131}	44.1 ± 0.2	< 5.3

Discussion

The spectra of the methyl substituted lipid series both clarify the use of the Raman C–H and C–C stretching mode regions for monitoring membrane matrix changes and illustrate several novel packing arrangements available to the diether-linked lipids. Thus, for example, the I_{2935}/I_{2882} and I_{2847}/I_{2882} peak-height intensity ratios provide temperature profiles for determining gel to liquid-crystalline phase-transition temperatures, T_m, and for assessing relative gel and liquid-crystalline order. Although both sets of indices are derived from the congested and complex 2900 cm^{-1} C–H stretching mode contours, it is usually accepted that the temperature curves constructed from I_{2847}/I_{2882} ratios reflect more directly changes in lateral chain–chain interactions, while the I_{2935}/I_{2882} ratios superimpose to varying extents the effects of *trans/gauche* isomerization upon the interchain perturbations [12]. These subtleties arise as a consequence of two molecular effects contributing to an alteration in the intensities of the methylene symmetric stretching modes centered about 2847 cm^{-1}. One perturbation to the intensity, manifest particularly in linewidth changes, originates from lateral, interchain Fermi resonance effects; the second intensity reorganization results from an intrachain Fermi resonance involving an interaction with the manifold of methylene bending mode overtones. Although the I_{2935}/I_{2882} ratio sensitivity reflects relatively small overall changes in bilayer reorganizations, the respective contributions from the two inter- and intramolecular effects can be difficult to deconvolute. We observe, however, in the present methyl-substituted ether lipid series that a distinct correlation exists between the I_{2847}/I_{2882} and I_{2935}/I_{2882} order/disorder parameters for the gel phase and ΔT, the gel to liquid-crystalline phase-transition cooperativity index. In arranging the lipid series in terms of increasing disorder within the gel phase, namely, 2-Me-DHPC < 3-Me-DHPC < 1-Me-DHPC, the I_{2847}/I_{2882} index yields profiles with ΔT values of < 1.5, < 1.9 and < 4.1 Cdeg, respectively. Analogously, for the curves derived from the I_{2935}/I_{2882} parameters, the ΔT values are 1.2 ± 0.1, < 1.4 and 2.2 Cdeg, respectively. As one may expect, the more ordered the gel phase in terms of a more tightly packed lattice (Figs. 2 and 3), as reflected by the intensity ratios, the smaller is the value of ΔT (viewed as a trend) and the more cooperative is the phase transition. (DHPC, the unsubstituted parent system, however, appears to be anomalous; we shall return to this point later.) We note, however, that the values for ΔT (again, viewed as a trend) are uniformly smaller for the curves derived from the I_{2935}/I_{2882} parameters compared to those constructed from the I_{2847}/I_{2882} ratios. Since these are statistically robust analyses [13], we consider the differences in ΔT to be real and not arising from artifacts of the analytical fitting procedure. These data therefore reinforce the notion that the two sets of empirical peak-height intensity ratios derived from overlapping spectral intervals within the C–H stretching mode region reflect molecular information of differing structural and dynamical origins. Further quantitative analyses would require a clearer knowledge of the overlapping band shapes contributing to the overall 2900 cm^{-1} spectral region.

An analysis of the thermotropic behavior of bilayer systems in terms of a two-state model using Raman spectral intensities yields the following expression for the effective domain size N_{eff} undergoing the gel to liquid-crystalline phase transition: $N_{eff} = 4RT_m^2/\Delta H_{VH}\Delta T$, where R is the gas constant and ΔH_{VH} is identified with the van't Hoff enthalpy implicit in the details of the order/disorder phase transition of the lipid hydrocarbon chains [13,14]. If we assume that the cooperative unit size is equivalent for interchain spreading and for *trans/gauche* isomerization; that is, if these events occur concomitantly, then the smaller values for ΔT derived from the I_{2935}/I_{2882} profiles, as discussed above, are consistent with the energetics of, for example, DPPC phase transitions. Thus, because of the inverse nature between the $\Delta H_{VH}\Delta T$ terms, the comparatively smaller transition breadths derived from the I_{2935}/I_{2882} curves associate greater van't Hoff enthalpies for the processes involving both inter- and intrachain disordering effects. For the 2-Me-, 3-Me- and 1-Me-DHPC series the C–H stretching mode region profiles suggest that the ratio (ΔH_{VH} (interchain) + ΔH_{VH} (*trans/gauche*))/ΔH_{VH} (interchain) is approx. 1.2, 1.4 and 1.9, respectively. In comparison, for the DPPC phase transition, Nagle [15] estimates

this ratio from intermolecular and thermodynamical considerations as approx. 1.5. We emphasize, however, that because of the relatively large temperature intervals between points (about 1.5–2 Cdeg), the ΔT values are of perhaps limited accuracy. A temperature interval of 0.1 ± 0.02 Cdeg, which is beyond the present capabilities of our intrumentation, is required to refine these points further.

Since the temperature profiles derived from the I_{1086}/I_{1131} peak-height intensity ratios provide a more direct estimate of intrachain *trans/gauche* isomerization, the values of ΔT in Table I yield ratios of ΔH_{VH} (interchain)/ΔH_{VH} (*trans/gauche*) for the phase transitions of 2-Me- and 1-Me-DHPC of about 1.4 and 2.0, respectively. These values are to be compared to a value of approx. 2.0 for DPPC [15]. The derived ΔT for 3-me-DHPC appears inconsistent with the values for the other substituted ethers, perhaps, because of the anomalous behavior of the gel-phase profile near the beginning of the phase transition (see Fig. 4). In summary, we observe that the transition breadth values for the methyl substituted systems are, in general, qualitatively consistent with the two-state model for a gel to liquid-crystalline phase transition. Again, further quantitative characterization of the phase transition by Raman spectroscopy require data determination at smaller intervals (e.g., 0.1 Cdeg). Data obtained at this precision should also allow tests and refinements of more detailed structural models to be more accessible.

Although the temperature-profile data for the methyl-substituted DHPC dispersions show little change from one ascending scan to another, the parent compound DHPC displays a somewhat anomalous effect (compare data in Ref. 3 and Table I) in that both the order/disorder characteristics in the gel and liquid-crystalline phases and the transition breadths vary significantly for a given sample cycled repetitively and slowly through its phase transition. Fig. 5 presents pure DHPC in its liquid-crystalline form at 46°C in (a) after one slow passage through the gel and liquid crystalline states and in (b) after several such cycles. The temperature scan rates are 3–4 Cdeg/h. A marked difference is observable between the degree of ordering for the two forms. It appears that after repeated slow warming and cooling cycles, the sample becomes more ordered in both phases above and below the main transition with the effect being more pronounced in the liquid-crystalline form, as shown in Fig. 5B [3]. The origin of this effect may be associated with the amount of bound water in the head-group region of the phospholipid [3]. Slow recycling of the unsubstituted diether lipid through its phase transition may alter the amount of water associated with the head-group. We suggest that an increased lattice order as a result of a tighter alkyl chain packing occurs as the head-group hydration spheres contract and the hydrocarbon chains complete their interdigitation. Since the substituted species experience some degree of head-group expansion as a consequence of the methyl groups in the interface region, the energetics favoring head-group dehydration are not as favorable. DPPC does not exhibit the analogous DHPC-ordering behavior on slow recycling through the phase transition, possibly because of the space-filling role of the acyl chain carbonyl groups. An additional consideration, however, may be that charge effects between water molecules and, particularly, the more exposed *sn*-2 chain carbonyl group are critical in precluding a general head-group dehydration effect in DPPC. We note that the acyl chains of DPPC interdigitate on dispersal of the diacyl phospholipid in glycerol [16,17].

Figs. 2 and 3 show that methyl substitution at the C(1) glycerol position leads to the maximum disorder for the series in both the gel and liquid-crystalline states. This behavior is expected if we assume the inequivalent hydrocarbon chain architecture demonstrated in diacyl phospholipids [18]. Substitution of a bulky methyl group at the 1-position of the glycerol backbone perturbs chain-chain correlations by separating the upper regions of the hydrocarbon chains. Since the ether linkage is flexible, the introduction of void volume within the bilayer would lead to an increase of *gauche* conformers along the chain (see Fig. 4) and increase the bilayer disorder reflected by Figs. 2 and 3. Substitution, however, of a methyl group at the 3-position of the glycerol moiety leads to a somewhat enlarged head-group region which, in turn, would alter the head-group packing characteristics. Perturbations to the conformational and

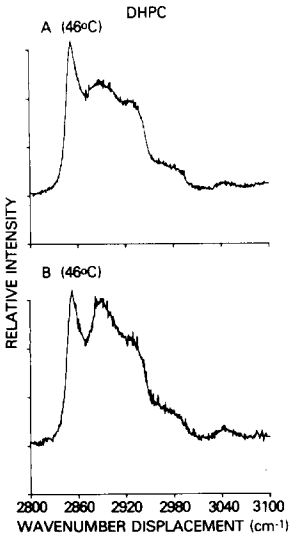

Fig. 5. Raman spectra in the C–H stretching mode region of two polymorphic forms of DHPC in the liquid-crystalline phase. (A) Spectrum obtained after first dispersing DHPC in water, cooling and recording one ascending temperature profile. (B) Spectrum obtained after multiple temperature scans cycling through the gel to liquid-crystalline phase transition. Note the appearance of a more ordered liquid-crystalline bilayer in (B).

packing arrangements within the head-group and interface regions are propagated into the hydrocarbon chains and are reflected in chain-packing reorganizations within the hydrophobic portion of the bilayer [19]. From an examination of space-filling models, the bilayer disruption from the 3-methyl substitution, however, would not be expected to be as severe as the 1-methyl substitution, consistent with the spectral observations. Examination of the lipid structure for a methyl substitution at the 2 position of the glycerol backbone suggests that no serious bilayer disruption, in comparison to DHPC, for example, would occur. That is, the methyl group lies in a plane nearly perpendicular to the hydrocarbon chain axis and is to some extent isolated from both the chain and head-group portions of the phospholipid; thus, we expect 2-Me-DHPC to exhibit the most ordered bilayer of the substituted series, as reflected by Figs. 2 and 3.

Although the 3-Me-DHPC derivative exhibits an increased gel-phase disorder compared to the 2-Me-DHPC dispersion (Figs. 2 and 3), the latter, well-ordered bilayer system undergoes its gel to liquid-crystalline phase transition at a slightly lower temperature (see Figs. 2–4 and Table I). Since ^{13}C-NMR data associate a conformational change at specifically the *sn*-2 carbonyl of acyl lipids with phospholipid phase changes [20], as well as within the interface region [21], we speculate that the presence of the methyl group at the 2-position is capable of altering the torsional barriers and twist angles involving the glycerol backbone and the ether linkage of the *sn*-2 chain. The resulting changes in the chain energetics may cause the lower value of T_m. Here we again assume inequivalent ether-linked chains analogous to the acyl systems [18]. It is thus evident that the degree of ordering in either the gel or liquid-crystalline phases of this lipid series is not necessarily predictive of the phase-transition temperature.

As noted above, the details of the gel and liquid-crystalline order/disorder characteristics of DHPC are related to its sample history (see for example, Figs. 2 and 3 and Fig. 2 in Ref. 3). Although the dotted temperature profiles for DHPC in Figs. 2 and 3 reflect a gel-state order comparable to that for 3-Me-DHPC, some DHPC dispersions reflect the high order assumed by the 2-Me-DHPC bilayers [3]. Since X-ray determinations indicate an interdigitated chain bilayer for DHPC [8], the comparable I_{2847}/I_{2882} values for the 2-Me-DHPC dispersions and the ordered forms of DHPC suggest an interdigitated structure for this specifically methyl-substituted diether. The gel-phase I_{2847}/I_{2882} intensity ratios for 1-Me- and 3-Me-DHPC dispersions clearly indicate non-interdigitated bilayer gel phases [17].

Finally, we observe that for the two ether lipids forming interdigitated bilayer dispersions, 2-Me-DHPC and DHPC, only DHPC possesses a pretransition as sensed by the Raman spectral parameters. Since the pretransition is generally associated with tilted gel-phase chains, a change in the interface region twist angles induced by the substitution at the 2-position may allow a chain packing arrangement to form which precludes the usual tilt that is characteristic of phosphatidylcholine systems.

Acknowledgments

We are grateful to Dr. Niels M. Witzky for his synthetic expertise. This work was supported in

part by a grant from the National Institutes of Health (HL16660).

References

1 Snyder, F. (ed.) (1972) Ether Lipids: Chemistry and Biology, Academic Press, New York
2 Paltauf, F. (1983) in 'Ether Lipids' (Mangold, H.K. and Paltauf, F., eds.), pp. 309–353 Academic Press, New York
3 Levin, I.W., Keihn, E. and Harris, W.C. (1985) Biochim. Biophys. Acta 820, 40–47
4 Bittman, R., Clejan, S., Lund-Katz, S. and Phillips, M.C. (1984) Biochim. Biophys. Acta 772, 117–126
5 Bittman, R., Clejan, S., Jain, M.K., Deroo, P.W. and Rosenthal, A.F. (1981) Biochemistry 20, 2790–2795
6 Hauser, H. (1981) Biochim. Biophys. Acta 646, 203–210
7 Lee, T-C. and Fitzgerald, V. (1980) Biochim. Biophys. Acta 598, 189–192
8 Ruocco, M.J., Siminovitch, D.J. and Griffin, R.J. (1985) Biochemistry 24, 2406–2411
9 Levin, I.W. (1984) in 'Advances in Infrared and Raman Spectroscopy' (Clark, R.J.H. and Hester, R.E., eds.), Vol. 11, pp. 1–48, Wiley, New York
10 Lord, R.C. and Mendelsohn, R. (1981) in 'Membrane Spectroscopy' (Grill, E., ed.), pp. 377–426, Springer-Verlag, New York
11 Witzke, N.M. and Bittman, R. (1985) J. Lipid Res. 26, 623–628
12 Huang, C.-H., Lapides, J. and Levin, I.W. (1982) J. Am. Chem. Soc. 104, 5926–5930
13 Kirchhoff, W.H. and Levin, I.W.
14 Sturtevant, J.M. (1974) Annu. Rev. Biophys. Bioeng. 3, 35–50
15 Nagle, J.F. (1980) Annu. Rev. Phys. Chem. 31, 157–195
16 McDaniel, R.V., McIntosh, T.J. and Simon, S.A. (1983) Biochim. Biophys. Acta 731, 97–108
17 O'Leary, T.J. and Levin, I.W. (1984) Biochim. Biophys. Acta 776, 185–189
18 Pearson, R.h. and Pascher, I. (1979) Nature 281, 499–501
19 Bush, S.F., Adams, R.G. and Levin, I.W. (1980) Biochemistry 19, 4429–4436
20 Wittebort, R.J., Blume, A., Huang, T.-H., Das Gupta, S.K. and Griffin, R.G. (1982) Biochemistry 21, 3487–3502
21 Fuson, M.M. and Prestegard, J.H. (1983) Biochemistry 22, 1311–1316